



Chitosan: Polyvinyl alcohol based mixed matrix sustainable coatings for reusing composite membranes in water treatment: Fouling characterization

Andrea Torre-Celeizabal^{*}, Aurora Garea, Clara Casado-Coterillo

Department of Chemical and Biomolecular Engineering, Universidad de Cantabria, Av. Los Castros s/n, Santander, Cantabria 39005, Spain

ARTICLE INFO

Keywords:

Chitosan
Polyvinyl alcohol
Layered silicates
Mixed matrix composite membranes
Fouling characterization

ABSTRACT

This work aims at studying the potential of modifying the surface of used polyamide (PA) reverse osmosis (RO) commercial membranes by coatings made of renewable and biodegradable polymers, chitosan (CS) and polyvinyl alcohol (PVA), filled with Cu-ion-exchange layered AM-4 titanasilicate and UZAR-S3 stannosilicate to provide antifouling properties and enlarging life time of thin-film composite (TFC) membranes. The water permeation and fouling ratios were evaluated as a function of active layer material in the presence of model organic (BSA) and inorganic (NaCl) foulants. The mixed matrix membrane (MMM) coatings added on the active surface of the PA commercial membranes generally decreased the flux decline and increased the permeate flow recovery rate. The CS:PVA based coatings promote the reversible and not the irreversible fouling, especially CuAM-4CS:PVA. Beside, ATR-FTIR confirms the reversible nature of the BSA fouling and the irreversible nature of the NaCl fouling. These results may in the future open the possibility of renewing the useful lifetime of commercial RO membranes by a simple coating method in the light of the circular economy.

1. Introduction

The constant growth of the world's population, accompanied by urban and industrial development, different periods of droughts, as well as industrial pollution, lead to an excessive demand of drinking water resulting in the absence of water resources. Moreover, simply storing rainwater is not enough to preserve and protect water resources, whose quality is aggravated by industrial and domestic pollution and other alternatives are required [1,2]. One possibility is membrane technology, as it is a separation process based on obtaining pure water suitable for human consumption in a sustainable way using pressure as a driving force [3].

The membranes used at commercial level are usually formed by different polymeric materials, mainly polyamide (PA) [4], cellulose acetate (CA) [5] or Teflon (PTFE) [6]. However, the major drawback of membrane technology is fouling, which is usually defined as a phenomenon involving undesirable accumulation of different solutes on the outside of the active surface of the membrane or inside the pores due to the complex physical and chemical interactions between different fouling agents present in the feed and the membrane surface itself, limiting the useful lifetime of the membrane and imposing costs related to frequent cleaning [1,3,7–11]. This implies a loss of productivity as

well as an increase in processing costs [12]. In this way, depending on the facility of cleaning this effect can be reversible, when foulants can be easily removed through physical washing and irreversible, when chemical procedures are required [10,11,13–16].

The literature on the “fouling” of membranes for water treatment has increased over-exponentially in the last decades. A search in Scopus database in the time period 1980 – 2020 with the keywords “fouling” and “membrane” or “membrane technology” returns almost 15,000 references, more than 90% of which are research articles. A general search on “membrane fouling characterization” without quotation marks in the same period gives back over 1600 references. However, many of the earliest works do not present any attempt to systematize the method for characterizing the fouling or antifouling behavior of the membranes, and thus in this work we restricted the search for the “fouling characterization” in “membranes” only returns 65 references in this period, as collected in Fig. 1. This may exclude other references such as membrane bioreactors in biogas upgrading or milk effluent valorization, where fouling is a major challenge as well, but the fouling characterization analysis attempted in this work would benefit those other applications in the future.

In particular, the surface modification of thin film composite (TFC) membranes has been attempted by grafting with another polymer

^{*} Corresponding author.

E-mail address: torrea@unican.es (A. Torre-Celeizabal).

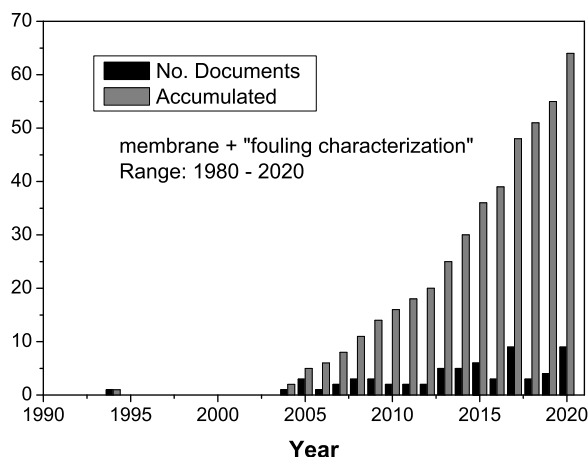


Fig. 1. Accumulated publication output for the “fouling characterization” or “membranes” not “MBR” (red) and the yearly published documents (black). (For interpretation of the references to color in this figure legend, the reader is referred to the web version of this article).

enhancing graft density and hydrophilicity to increase water flux and reduce foulant adhesion [17], by the hybridization of the thin film PA layer by introducing different fillers on the external skin of PA TFC membranes, such as TiO_2 [18,19], Cu-exchanged ferroxides [20,21], bio-inspired graphene oxide derived fillers [22,23], among others. The incorporation of inorganic compounds embedded in polymer matrices, having as a result a mixed matrix membrane (MMM) [13,24,25], coated onto the external selective layer of the membrane, is one of the preferred surface modification method of membranes in water and other applications [26–28] to reduce the effect of fouling by tuning the hydrophilicity to reduce the effect of concentration polarization and increase the lifetime of the membrane [29–31]. Beside the compatibility with the porous support, attention should be paid to the prevention of release of toxic components to water for human consumption throughout the useful lifetime of the membrane process [32]. Copper is a commonly studied material in antifouling coatings due to its availability, hydrophilicity inducement, low cost and thermal conductivity, as well as high biocidal capacity, but it has a big disadvantage, which is that copper nanoparticles in water are toxic for humans [33]. Antifouling approaches should guarantee conditions where the migration of free copper ion and nanoparticles to water are below the WHO threshold [34].

Therefore, coating mixed matrix membrane (MMM) materials containing advanced structures such as zeolites [25], ion-exchanged zeolites [35,36], metal organic framework [37] and zeolitic imidazolate frameworks [37,38] fillers have been extensively reported in dense and TFC configuration. The antifouling ability of the membranes is increasingly attempted by an increasingly systematic characterization of fouling ratios and indexes to establish the antifouling performance in the state-of-the-art research and technology reports [39,40]. The antifouling properties of the TFC membranes are usually characterized using two of the most common model foulants, bovine serum albumin protein (organic) [5,17,22,41–43] and NaCl salt (inorganic) [8,23,44]. The understanding of fouling mechanisms in biopolymer modified membranes leaves still much room for improvement [45].

In light of the circular economy, attention is recently turned to the use of non-toxic or renewable materials for membrane fabrication and modification, to enlarge the useful lifetime of existing membranes and the replacement intervals and lower the cleaning costs [46]. Chitosan (CS) is a low cost, biocompatible, hydrophilic and non-toxic biopolymer derived from abundant natural and renewable sources (chitin), with good film forming but low mechanical resistance that can be improved by blending with biodegradable poly (vinyl) alcohol (PVA) [47]. The metal adsorptive properties of CS allow expecting a low migration of toxic compounds to the water effluent [33,48].

MMM layers made of an CS:PVA equimolar blend filled with Cu-exchanged layered AM-4 and UZAR-S3 layered silicate fillers, whose tunable hydrophilicity, mechanical strength and the ability to preserve the copper oxidation state and the preservation of this component within the polymer matrix has been observed in a previous work [49]. This work aims at evaluating the experimental characterization of the antifouling properties of such MMM layers on fresh and used RO PA TFC membranes in order to evaluate the potential of a simple modification procedure based on sustainable materials to enlarge the useful lifetime of commercial composite membranes.

2. Materials and methods

2.1. Materials

Commercial PA RO membranes were obtained from GE Infraestructure Water & Process technologies (USA). The two polymers used for the coatings, chitosan (CS) and polyvinyl alcohol (PVA) were both purchased from Sigma Aldrich (Spain). For the synthesis of the two nanoporous silicates sodium silicate (Na_2SiO_3), sodium hydroxide (NaOH), Anatase (TiO_2), tin(II) chloride di-hydrated ($\text{SnCl}_2 \cdot 2\text{H}_2\text{O}$) and copper chloride $\cdot 5\text{H}_2\text{O}$ were acquired from Aldrich (Spain). Other reagents that have been used for membrane preparation are acetic acid (glacial, Panreac) for CS solutions, sodium hydroxide pellets (Panreac, Spain), H_2SO_4 (Panreac, Spain), glutaraldehyde (GA, Sigma Aldrich), in order to prepare post-treatment solutions and NaCl (Panreac, Spain), and BSA (Sigma Aldrich, Spain) to prepare the model foulant solutions.

2.2. Membrane preparation

The laminar silicates have been synthesized by an optimized hydrothermal synthesis method without organic surfactants and ulterior copper ion exchange with $\text{Cu}(\text{NO}_3)_2$, as reported elsewhere [49–51]. The polymer solutions were prepared by dissolution in aqueous solvents, CS 1 wt.% in 2 wt.% acetic acid and stirred at room temperature, while PVA 4 wt.% was dissolved in distilled water, under stirring and reflux at 80 °C. After 24 h, polymer solutions were filtered in order to remove any residual impurities, before being mixed into an equimolar blend, CS:PVA 50:50 mol%, which was the most stable according to previous works [49,52] and stirred for another 24 h to ensure an homogenous mixture.

In the case of the MMMs, the fillers were added at this point to the polymer blend, at a loading of 10 wt.% with respect to the total solid content [49]. This value was selected in previous studies for the hydrophilic and mechanical properties provided to the MMMs imparted to the membranes in order to evaluate the effect of the type of filler on the antifouling properties, which is the purpose of the present work. The dispersion was further stirred 24 h to homogenization. The coating was carried out on the selected substrate (new or re-used PA membrane) using a doctor blade with an opening of 0.150 mm. Solvent was evaporated after 24 h in a fume-hood at room temperature (20 °C). The membrane was activated by immersion in a NaOH 1M bath for 1 h and then thoroughly rinsing the excess hydroxide with water.

Before being coated, all the RO membranes used in this study were submerged in deionized water for 24 h in order to eliminate the possible excess of components that could be in the active surface of the membranes. Later, the coatings were carried out as described above.

In order to improve mechanical strength and integrity of the coated layers, additional chemical crosslinking was performed, either by immersing the activated membranes in a H_2SO_4 0.01 M aqueous solution bath or a 0.25% glutaraldehyde solution in water [53], followed by rinsing in water to remove the excess acid or crosslinker before filtration experiments.

2.3. Characterization of the hydrophilicity of thin film composite membranes

Pure water permeability. The filtration performance of the membranes was characterized in a SEPA CF II test equipment (Osmonics), consisting of a membrane cell of 140 cm² effective area, connected to a centrifugal pump with a 200 L tank filled with DI water (18.2 MΩ) in order to perform the water filtration characterization of the fresh membranes in steady state conditions. The pressure was set at a fixed value between 40 and 5 bar, and the system was left to homogenize for 15–30 min. The value of the pure flux of water, J_w , in units of L m⁻²h⁻¹ was obtained by Eq. (1)

$$J_w = \left(\frac{V}{A \times \Delta t} \right) \quad (1)$$

where A is the membrane surface area (m²), V (L) is the volume of the collected permeate, Δt is the filtration time (h) and J_w is the flux of water, expressed in LMH (L m⁻² h⁻¹). In order to observe the relationship with the transmembrane pressure, TMP (bar), the pressure was decreased following identical procedure.

Water uptake (WU). This parameter was calculated from the difference of weight of the hydrated membranes (W_{wet}) and dry membranes (W_{dry}), measured in an electronic balance. The dry weight was obtained directly from the membrane after the crosslinking treatment and the wet weight after immersing the membrane in deionized water for 24 h at room temperature, subsequently removing excess water on the surface with blotting paper. Eq. (2) was used to calculate the WU of the commercial uncoated membrane,

$$WU (\%) = \left(\frac{W_{wet} - W_{dry}}{W_{dry}} \right) \times 100 \quad (2)$$

while for the WU of the CS:PVA based composite membranes it was necessary to use Eq. (3), in order to correct the influence of PVA by adding the term of the density of water (1.0) and PVA (1.3) [54] as,

$$WU (\%) = \left(\frac{\frac{W_{wet} - W_{dry}}{1.0} - \frac{W_{dry}}{1.3}}{\frac{W_{dry}}{1.3}} \right) \times 100 \quad (3)$$

Swelling degree (SD). To determine the dimensional swelling capacity of the membranes studied, the thickness of layers was measured both wet (D_{wet}), after immersion for at least 24 h in water, and removing the excess moisture with blotting paper, and dry (D_{dry}), using a Mitutoyo IP-65 micrometer in different spots of the membrane area, obtaining the swelling percentage by Eq. (4) [55],

$$SD (\%) = \left(\frac{D_{wet} - D_{dry}}{D_{dry}} \right) \times 100 \quad (4)$$

Surface chemical characterization. The ATR-FTIR technique is the usual tool to determine the chemical properties of RO membranes that can give evidence of the functional groups present both on the surface and in a given depth, depending on the angle of incidence, as well as the number of incident waves. For this characterization the equipment used is the GladiATR Spectrum 65 FTIR spectrometer (PIKE technologies, US). In order to observe the changes in the surface of the different membranes, this technique was used before fouling, after this phenomenon and finally, after the washing procedure.

2.4. Fouling characterization experiments

In this work, the fouling experiments have been carried out in the same filtration equipment described in Section 2.2, but changing the 200 L tank by two tanks of 20 L with either tap water to accelerate the deterioration of the membrane and those containing different foulant compositions to be fed to the system consecutively as explained below. First, synthesized membranes were pressurized with tap water at 5 bar

for 30 min to achieve a steady state previous to the characterization. In the next step, pure water was allowed through the membrane to obtain the value of $J_{w,1}$ by Eq. (1), in the range of 5–15 bar to complete the previous characterization as in the study of Zareei and Hosseini [20].

The filtration experiments were carried out in the presence of two model foulants, one organic (BSA) and another one inorganic (NaCl) to evaluate the antifouling properties. For this purpose, solutions of 0.1 g/L BSA [5,16,21,41,56] and 0.1 M NaCl [6,14,20] were prepared in a 10 L tank each separately. These experiments were carried out by setting the TMP at 3 bar and an ambient temperature of 22 °C for 90 to 120 min for each of the foulants. Permeate and retentate samples were taken in the same conditions as before, and then a second value of flux was obtained, $J_{w,p}$.

The concentration of permeate and retentate samples during the initial characterization has been measured with a conductivity meter. With these values, by performing a previous calibration with known concentration patterns, it has been possible to calculate the rejection of the synthesized membrane to the foulants using Eq. (5),

$$R(\%) = \left(1 - \frac{C_p}{C_f} \right) \times 100 \quad (5)$$

where C_f is the concentration of the foulant in the feed and C_p is the concentration of the foulant in the permeate.

The resistance to fouling was determined after carrying out the experiments in pure and tap water, once the membranes are washed with abundant water and immersed in water for 24 h before the third filtration experiment that allowed us obtaining a third water flow value, $J_{w,2}$. This is carried out by filtration for 120 min. Now the flux recovery ratio (FRR) and flux decline (FD) can be calculated by Eqs. (6) and (7), respectively,

$$FRR(\%) = \left(\frac{J_{w,2}}{J_{w,1}} \right) \times 100 \quad (6)$$

$$FD(\%) = \left(1 - \frac{J_{w,p}}{J_{w,1}} \right) \times 100 \quad (7)$$

As mentioned before, from these experiments it is also possible to calculate the fouling process that occurs on the surface of the membrane, which can be reversible when fouling agents are weakly attached to the membrane, or irreversible when fouling agents adhere strongly to the active surface of the membrane, due to physical or chemical interactions between them. In this way, the reversible, irreversible, and total fouling ratios are defined in Eqs. (8), (9), and (10), respectively.

$$R_r(\%) = \left(\frac{J_{w,2} - J_{w,p}}{J_{w,1}} \right) \times 100 \quad (8)$$

$$R_{ir}(\%) = \left(\frac{J_{w,1} - J_{w,2}}{J_{w,1}} \right) \times 100 \quad (9)$$

$$R_t(\%) = \left(1 - \frac{J_{w,p}}{J_{w,1}} \right) \times 100 \quad (10)$$

where R_r , R_{ir} and R_t are the reversible, irreversible and total fouling ratios contribution to fouling.

3. Results and discussion

3.1. Characterization of the hydrophilicity of the composite membranes

The water permeability coefficient that characterizes a thin film composite membrane can be obtained from the slope of the linear relationship between the water permeate flow rate (LMH) and the TMP [57]. The linearity of the relationship between water flux and transmembrane pressure observed for the freshly prepared membranes confirms observations for chitosan films reported in literature [58]. The

evolution of pure water flux vs TMP is plotted in Fig. S1 in the supporting information and the water permeability coefficients calculated from the slope of those curve, in terms of $\text{L m}^{-2}\text{h}^{-1}\text{bar}^{-1}$ are collected in Table 1. The highest average water permeability coefficient was obtained for the CuAM-4CS:PVA coating layer, which could be attributed to the high affinity for water of AM-4 layered titanosilicate [59]. This high hydrophilicity also stands for by the standard deviation at higher TMP observed in Fig. S1(c), at the Supporting information. On the other hand, the membrane with the lowest water permeability coefficient was the one with CuUZAR-S3/CS:PVA coating, which could be related to the fact that the distribution of the sheets of this laminar stannosilicate has generated a barrier that prevents the flux of water. The fitting parameter R^2 for the PA membrane was too low to provide an accurate water permeability value, and it was included here only to give an order of magnitude.

The fresh membranes were characterized regarding their WU, SD, and the results are collected in Table 2.

The hydrophilic character of the membranes can be confirmed by measuring the water adsorption capacity calculated by Eqs. (2) and (3), values collected in Table 2. The water uptake (WU) of the CuAM-4 loaded membrane layer, was higher than the others, indicating a higher affinity with water, above even the hydrophilic polyamide TFC commercial membranes [60]. The increase in hydrophilicity of the membrane surface has been reported beneficial not only to improve water permeation but also to reduce the fouling by organic hydrophobic foulants present in wastewaters [56]. Copper and silica oxide fillers have been added to commercial polymers to improve the hydrophilicity of the surface membrane layer, and this is usually monitored by water contact angle [61,62]. The water contact angle of CS-based MMMs loaded with hydrophilic titanosilicates provided values of the same range of magnitude as pure CS biopolymer, in a previous work with three dimensional hydrophilic ETS-10 titanosilicate as fillers [63].

The swelling dimensional capacity (SD), also collected in Table 2 and measured by the difference between the wet and dry thickness of the TFC membranes, has therefore been used as a measure of the mechanical resistance of the coated layer. The modified membrane with the highest swelling degree was the CuUZAR-S3CS:PVA/PA membrane, closer to the uncoated PA membrane, which usually indicates that it is prone to a higher deformation degree, which may translate in low mechanical resistance [49], similarly to the pure CS:PVA coated membrane.

Xie et al. highlighted the influence of WU and SD of the membranes in their performance and antifouling resistance of anion-exchange membranes in electrodialysis [44]. This confirms the hypothesis of this work that fouling characterization should be taken into account in other separations using membranes, given the transversality of the membrane materials and configurations in applications as diverse as water desalination and CO_2/CH_4 separation, as demonstrated recently by Ali et al., where they adjusted RO TFC membranes by interfacial polymerization to create defect-free selective membranes with improved selectivities in CO_2/CH_4 separation [28].

3.2. Evolution of water flow in the presence of foulants

The impact of the hydrophilicity of the coating layer on the stability of the water permeability was observed when calculating the water

Table 1
Water permeability coefficients of the fresh thin film composite membranes.

Membrane	Water permeability ($\text{L m}^{-2}\text{h}^{-1}\text{bar}^{-1}$)	R^2	Total thickness (mm)
PA	2.736 ± 0.869	0.748	0.124 ± 0.0014
CS:PVA/PA	1.705 ± 0.235	0.945	0.169 ± 0.0094
10CuAM-4CS:PVA/PA	2.745 ± 0.220	0.980	0.191 ± 0.0148
10CuUZAR-S3CS:PVA/PA	0.676 ± 0.044	0.987	0.217 ± 0.0166

Table 2

Water uptake (WU) and Swelling degree (SD) values of the membranes.

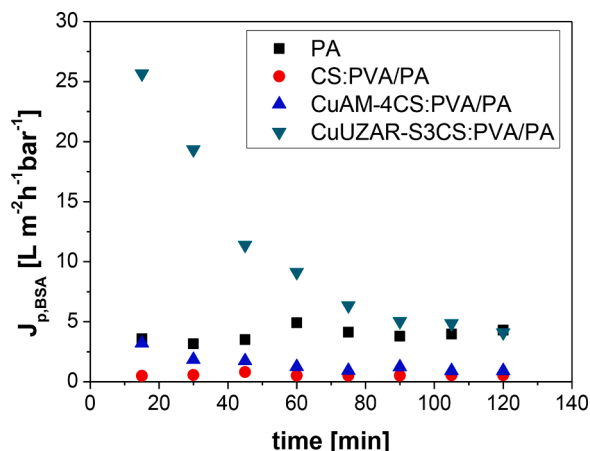
Membrane	WU (%)	SD (%)
PA	16.04	19.50
CS:PVA/PA	15.40	1.15
10CuAM-4CS:PVA/PA	19.84	9.35
10CuUZAR-S3CS:PVA/PA	13.77	17.52

permeability coefficient of the membranes when a second coating was made after a preliminary fouling experiment by immersion in concentrated BSA solution (0.1 g/L) and characterization by water filtration experiments observing a huge recovery of the water flux through the CuAM-4CS:PVA/PA membrane suggesting unfavorable protein adhesion in this membrane material [35]. The water permeability after the second coating on the used membranes gave values of $2.121 \pm 0.509 \text{ L m}^{-2}\text{h}^{-1}\text{bar}^{-1}$ and $2.0184 \pm 1.068 \text{ L m}^{-2}\text{h}^{-1}\text{bar}^{-1}$ for the CuAM-4CS:PVA/PA and uncoated PA membranes, respectively, obtained before the fouling experiments with tap water, as described at the beginning of Section 2.3. These water permeability values, were still very similar to the fresh membranes characterized in Table 1 with deionized water, while the water permeability coefficient of the CS:PVA/PA and CuUZAR-S3CS:PVA/PA composite membranes decreased and increased from the value obtained for deionized water, respectively. This is agreeing with the behavior observed regarding the lower mechanical resistance of these latter membranes observed in the swelling degree reported in Table 2.

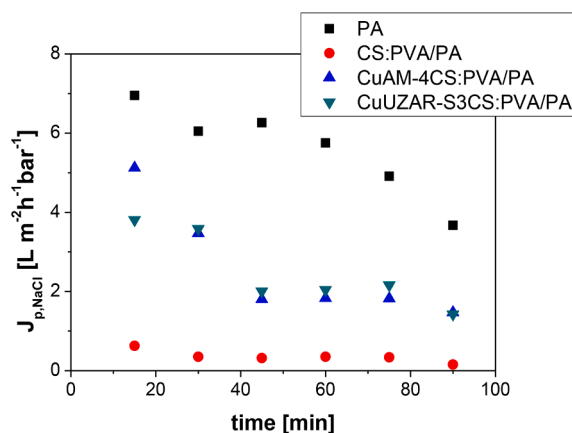
Fig. 2(a) and (b) represent the evolution of water flux of the re-used membranes after filtration fouling experiments in the presence of BSA organic foulant and NaCl inorganic foulant in the feed, at a TMP of 3 bar.

Considering the evolution of water fluxes for the different membranes, in the case of the uncoated re-used PA membrane, it was observed that the flux was lower in the presence of the protein foulant than in that of the inorganic foulant, but after the final washing, the water flux was recovered, pointing out that fouling in PA TFC membranes was a reversible process. With respect to the membrane coated by a CuAM-4/CS:PVA MMM layer, the effect of both fouling agents was observed to be very similar, but the water flux recovered noticeably after the final washing, indicating that fouling was reversible, in agreement with the highly hydrophilic nature of the CuAM-4 filler [49,62]. As hinted above, the effect of the pure CS:PVA and CuUZAR-S3CS:PVA coatings in the presence on the permeate flux was very similar in the presence of BSA or NaCl type of foulant. The final washing led to a further increase of the water flux through the CS:PVA membrane, as shown in Fig. 2(c), while water flux of the CuUZAR-S3CS:PVA MMM coated membrane was not recovered after the fouling experiments, which may be attributed to a stronger adhesion of the foulants on the CuUZAR-S3/CS:PVA MMM layer than in the other cases, perhaps due to the higher ion-exchange capacity of this material [49].

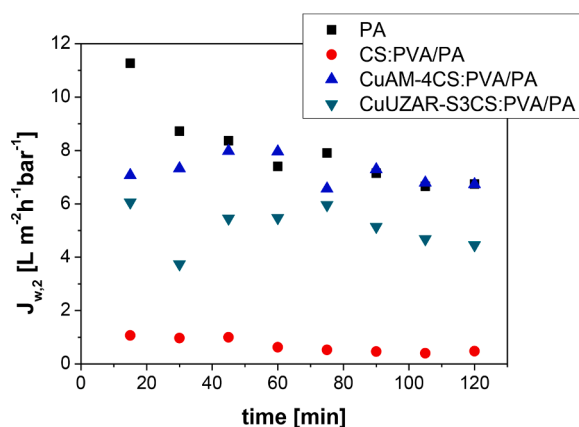
Fig. 3 represents the rejection of the foulants calculated using Eq. (5). In this case, the rejection of the organic foulant depends on the material of the surface layer of the coated membrane, exceeding the value of the uncoated membrane both membranes with the laminar silicates, although in all cases this value remains below 60%, which differs from the starting point of Saraswathi et al. who used a 1000 ppm BSA solution and observed BSA rejection increased from 85% to 99% with increasing amount of CuO nanoparticles embedded in PVDF [62], which may be related to the probable change in isoelectric point of the membranes by means of the MMM layer coating [41] or an irreversible effect of other use of the membranes [2]. For the NaCl inorganic foulant, the results were slightly lower on all the tested membranes compared with the commercial membrane, in agreement with literature [64]. This result is common in the MMM literature and it can be explained in terms of hydrophilic, ion exchange and mechanical properties of the coating material being enhanced by the presence of particles embedded in the polymer [49].



(a)



(b)



(c)

Fig. 2. Evolution of the flux of water through re-used membranes after second coating: (a) in the presence of BSA foulant, (b) in the presence of NaCl foulant and (c) after final washing with water at the end of fouling characterization.

The rejection of the organic and inorganic foulants were related to the WU and SD parameters in Table 2. The membrane with higher WU values showed higher BSA rejection, since WU is related to the affinity of the surface of the membrane with water, and the higher hydrophilic character makes it harder for the organic molecules to adhere to the surface of these membranes [56,65]. Therefore, it may be concluded

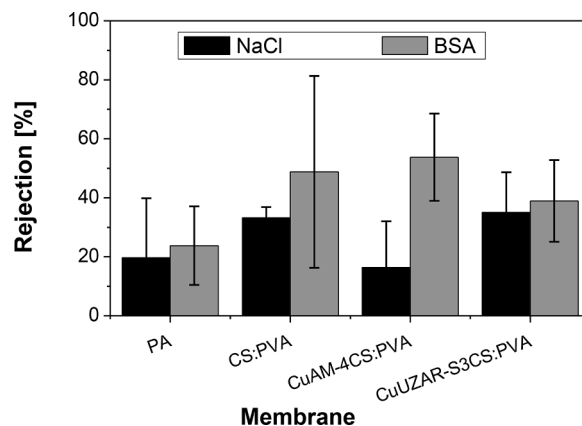


Fig. 3. Organic and inorganic model foulants rejection values for the different membranes studied in this work.

that the hydrophobic interaction between the organic foulant and the membrane surface is reduced by establishing a thin layer of water between them, reducing foulant adhesion [42].

The majority of the studies focus the fouling characterization on BSA fouling analysis. Thus, another parameter reported on the fouling resistance of the membranes to organic fouling is BSA rejection. In this way, membranes prepared by Rabiee et al. had a BSA rejection close to 90%, higher to the pristine polymer, meaning that TiO_2 addition reinforced BSA resistance of prepared membranes due to a lower affinity between the modified membrane surface and the BSA molecules [66]. Hu et al. reported that the addition of GO nanoparticles to PES/SPSf improved BSA resistance to almost 99%, which was explained by the electrostatic repulsion occurring between BSA molecules and the modified membrane surface as the cause of the increase in BSA rejection [67]. Nasrollahi et al. stated that fouling depended not only on the hydrophilicity of the membrane, but also on the surface roughness, pore size, pore size distribution and surface charge so that high surface roughness, large pore size, broad pore size distribution and high flux led to greater effect in membrane fouling. This caused that although they obtained a BSA rejection value close to 90%, the best membrane performance was provided by the membrane with an intermediate filler loading, in order to prevent agglomeration of filler particles in the modified layer [68].

In order to systematize the fouling characterization according to recent literature, the different fouling ratios and indexes are represented below.

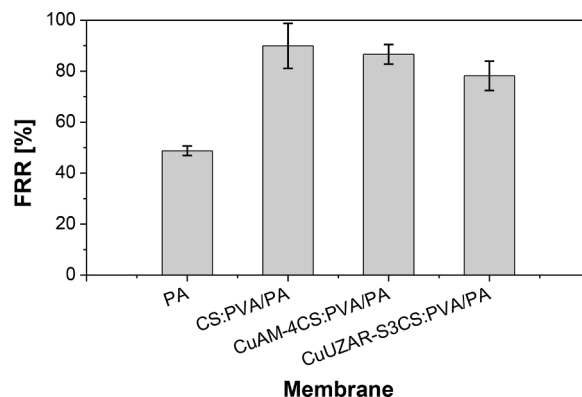


Fig. 4. Flux recovery rate (FRR) as a function of MMM coated layer composition.

3.3. Flux recovery ratio and flux decline

The results obtained for the flux recovery ratio (FRR) are represented in Fig. 4. A higher FRR value means a better antifouling behavior of the membrane, and usually also a higher productivity and longer service life [69]. In this work, the value of the uncoated PA membrane was lower than for the coated membranes, with values up to 50%. Neat commercial CA membranes reported FRR after fouling in HA solutions of 39–58% [69]. For the modified membranes the FRR exceeded values of 80%. The highest value was achieved for the CS:PVA/PA TFC membrane, close to 90%, which accounts to the increased hydrophilicity after the washing treatment of the pure biopolymer blend [17,22,23].

In Fig. 5, the Flux Decline (FD) is evaluated. FD indicates how the flux through the membrane was reduced after the whole fouling characterization test, therefore, the lower this rate the higher the resistance to fouling of the membrane [24]. Considering the results of Fig. 5, this rate was higher when the fouling agent used is organic except for the CuUZAR-S3CS:PVA coated membrane. This could be related to the WU and SD properties measured for these membranes and commented above. In general, the FD results agree with FRR observations in that the hydrophilicity of the pure polymer blend was recovered after the washing stage better than the MMM coated membranes.

Flux decline upon BSA fouling characterization of UF membranes modified by MMM approach oscillate in the range of 21% [23] and 28.6% [61], for GO-based MMM surface layer and ion-exchanged based zeolites-PES MMM, respectively, as a function of variable hydrophilic character of the membranes in terms of their composition.

Most of the studies focus the attention on the Flux Recovery Ratio (FRR) index of the membranes in water treatment. For example, Vatanpour et al. prepared nanocomposite polyethersulfone (PES) membranes with multiwalled carbon nanotubes (MWCNTs) coated by anatase titanium dioxide (TiO_2) nanoparticles and obtained an FRR of around 80%, somewhat 30% higher than the PES pristine membrane [70]. Later on, Rabiee et al. reported emulsion poly(vinylchloride)/ TiO_2 nanocomposite UF membranes via phase inversion and obtained a FRR of 75%, not much better than the uncoated EPVC membrane, which showed a FRR value of 69% [66]. Jamshaid et al. synthesized MMM of polyvinyl chloride-co-vinyl acetate/cellulose acetate (PVCA/CA) infused with zeolites by dissolution casting method for desalination and reported a FRR of 67% [71]. Hu et al. obtained a FRR of around 90%, where the addition of GO by preparing GO nanosheets -(PES)/sulfonated polysulfone (SPSf) MMMs by non-solvent induced phase separation, concluding that the addition of GO nanosheets improved the hydrophilicity and protein adsorption of non-treated membranes [67]. Singh et al. reported UF membranes modified by a MMM layer containing Cu_2O hydrophilic photocatalysts, with increasing FRR with increasing

Cu_2O content, while the BSA rejection decreased accordingly [72]. Nasrollahi et al. prepared copper oxide/PES UF membranes for water treatment and analyzed the fouling resistance of this membranes, obtaining an FRR of 60% a bit higher than the bare membrane [68]. For instance, those experimental data agree with the results presented in this study, in that the CS:PVA layer coatings induced a higher FRR, due to the increased hydrophilicity of the modified MMMs that could improve the resistance of the membrane to fouling.

3.4. Reversible and irreversible fouling ratio

As mentioned before, the reversible fouling refers to the one that is more easily recovered by simple washing conditions [50,73,74], while the irreversible fouling is taking place when the molecules of the foulant are strongly adhered to the materials in the membrane surface can only be removed through chemical treatments, often using costly reactants [5,12]. In the following figures both types of fouling ratio will be evaluated for the organic and inorganic model foulants studied in this work.

Fig. 6 shows the organic fouling characterization of the membranes studied in this work using BSA. Here, irreversible fouling was lower for the membranes coated with the MMM materials, containing the layered silicates CuAM-4 and CuUZAR-S3, respectively, in the CS:PVA blend matrix. This can be correlated with the translation of the hydrophilicity and ion-exchange capacities and porosity of the fillers to the hydrophilicity of the membranes, which makes the organic foulant molecules less susceptible of binding on the membrane surface [62]. The irreversible fouling index of PES UF membranes increased from 30 to 61% upon hybridization with GO [22]. In the same argumentative line, the reversible fouling increases exclusively for the membrane coated by the CuAM-4CS:PVA layer, which shows the highest total BSA fouling rate [17].

The characterization of inorganic fouling is represented in Fig. 7, regarding the results obtained in the presence of NaCl in the feed. Here, irreversible fouling was lower for the MMM coated membranes. The reversible fouling ratio in this case, was higher to all modified TFC membranes than the uncoated commercial membrane, which may be related to the relationship between the swelling degree and the hydrophilicity of the surface materials and the flux of water, as commented above [75].

3.5. ATR-FTIR surface observations

The ATR-FTIR technique is usually reported in fouling characterization literature for the characterization of surface modification membranes before any filtration experiments. In this work, we use this technique to observe the surface of the membranes before and after the

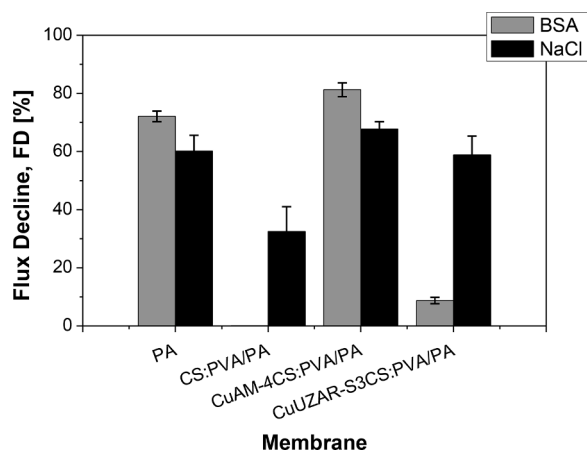


Fig. 5. Average flux decline values obtained after the experiments in the presence of organic and inorganic foulant for the different membranes.

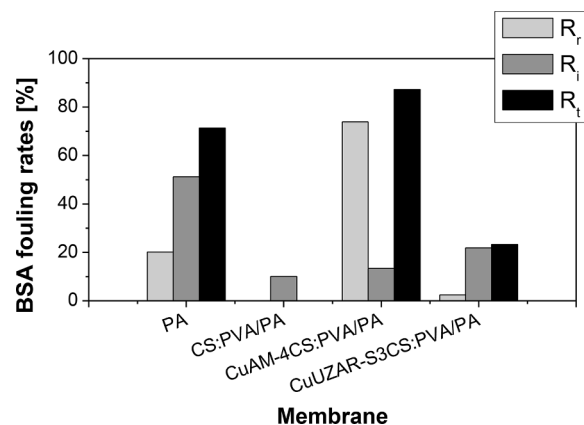


Fig. 6. Reversible (R_f , light gray), irreversible (R_i , gray) and total (R_t , black) fouling rates as a function of membrane layer composition when using BSA as model organic foulant.

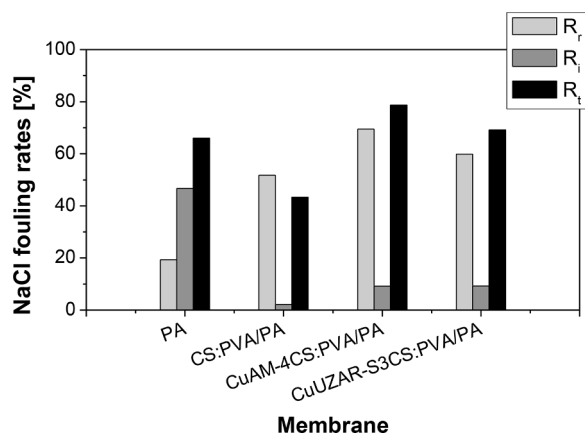


Fig. 7. Reversible (R_r , light gray), irreversible (R_i , gray) and total (R_t , black) fouling rates as a function of membrane layer composition when using NaCl as model inorganic foulant.

fouling test cycles. Fig. 8 shows the spectra obtained at the different stages of the fouling characterization procedure, that is, before, after fouling and after final washing with running water and the characterization of FRR. First observation withdrawn is the hydrophilicity of the membranes, represented by the bands at 3400 cm^{-1} , corresponding to the -OH functional group. This band decreases generally after fouling due to the grafting of BSA and then NaCl to the surface, especially for the CuUZAR-S3/CS:PVA MMM coated membrane, similarly to the re-used uncoated PA membrane, and less obvious for the CS:PVA and CuAM-4CS:PVA MMM coated membranes, which it is probably related to the different effects of swelling degree (SD) and water uptake (WU), respectively, as commented above (Table 2).

What is interesting, is the possibility to appreciate the peak attributed to the presence of BSA on the surface of the membrane at approximately 1640 cm^{-1} [55]. In the same way, the presence of the inorganic foulant, NaCl, is attributed to an additional peak at 1100 cm^{-1} . These values allow calculating the ratio of absorbance intensities of the bands at 3400 cm^{-1} and 1600 cm^{-1} for BSA and at 3400 cm^{-1} and 1100 cm^{-1} for NaCl, represented in Fig. 9 in order to characterize the presence of each foulant on the membrane surface [26]. These results also indicate a reduction in the adhesion of the foulant to the outer surface of the membrane, since it is possible to observe how the ratio decreases as the coatings are added.

Beside this, the presence of both foulants on the membrane surface

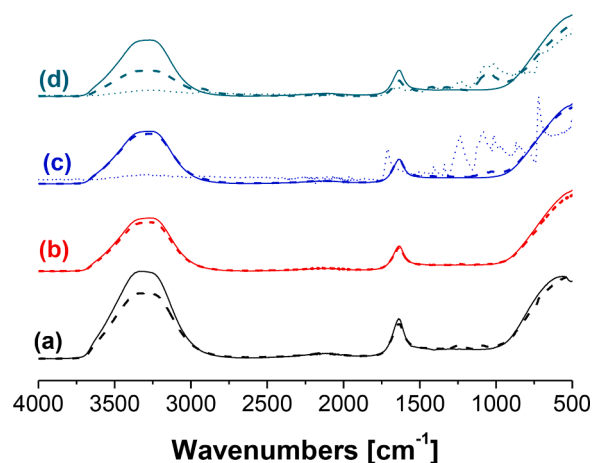


Fig. 8. ATR-FTIR of the GA crosslinked PA (a), CS:PVA/PVA (b), CuAM-4-CS:PVA/PA (c) and CuUZAR-S3-CS:PVA/PA (d) membranes, freshly made (thin lines), after fouling experiments (dashed thick lines) and after final water washing stage (dotted lines).

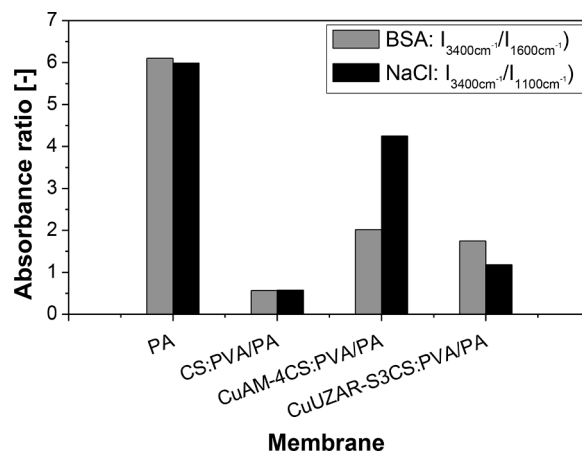


Fig. 9. Ratio of the band intensity at 3400 cm^{-1} to the band intensity for BSA (black) and NaCl (red) in the ATR-FTIR spectra for the membranes. (For interpretation of the references to color in this figure legend, the reader is referred to the web version of this article.)

confirms observations regarding reversible and irreversible fouling rates, because, when the appearance of the characteristic peaks in the spectrum appear after washing with water corroborates the existence of irreversible fouling, which is defined as that which cannot be eliminated by physical cleanings.

Table S1 collects the selected literature reports on mixed matrix membranes or surface modified composite membranes, prepared by a coating a polymer or mixed matrix layer on a porous support or another membrane. The selection is restricted to the recent works accounting for fouling characterization procedures that contributed to support the results obtained in this work. Remarkable it is that not all the works use all the fouling ratios simultaneously and most focus on the physicochemical and morphological observation by microscopy and spectroscopy techniques among others to hypothesize on the interaction between the surface of the membrane and the interaction with foulants. In fact, the use of irreversible and reversible fouling indexes is quite recent in membrane literature. Comparing the literature values with the ones obtained in our present study, we can confirm the potential of exploring both performance and fouling characterization of the sustainable CS:PVA-based sustainable MMM materials studied in this work since they managed to improved antifouling properties in line with other materials in literature.

4. Conclusions

This work deals with the surface modification method of new and re-used polyamide reverse osmosis membranes by a simple dip-coating of selected mixed matrix membrane (MMM) materials based on chitosan (CS) biopolymer and low-cost, biodegradable polyvinyl alcohol (PVA) hybridized with ion-exchanged layered silicates with tunable hydrophilic and mechanical properties, and the characterization of their fouling resistance in water treatment.

Fouling results revealed that MMM coatings added on the active surface of the PA commercial membranes generally decreased the flux decline and increased the permeate flux recovery rate. This was correlated with the increased reversible fouling to irreversible fouling contribution.

All these conclusions indicate that, by means of a simple sustainable surface modification of the membrane surface, it is possible to increase the performance of the membrane and enlarge its useful lifetime, by reinforcing reversible rather than irreversible fouling, facilitating the removal of foulants through simpler washing processes. Further work could be devoted to gain insight in the different grafting of inorganic and organic foulant onto the external surface of the membrane and the long-

term performance of these membranes in the treatment of other residual effluents.

Declaration of Competing Interest

The authors declare that they have no known competing financial interests or personal relationships that could have appeared to influence the work reported in this paper.

Acknowledgments

Financial support from the Spanish Ministry of Science and Innovation under project PID2019-108136RB-C31 /AEI/10.13039/501100011033. MCIN/AEI/10.13039/501100011033 and the “European Union Next Generation EU/PRTR” for the Grant EIN2020-112319/AEI/10.13039/501100011033 are gratefully acknowledged. The Early Stage Researcher grant PRE2020-09765, funded by MCIN/AEI/10.13039/501100011033, is also thanked (A.T.C.).

Supplementary materials

Supplementary material associated with this article can be found, in the online version, at [doi:10.1016/j.cej.2021.100236](https://doi.org/10.1016/j.cej.2021.100236).

References

- [1] D.J. Miller, D.R. Dreyer, C.W. Bielawski, D.R. Paul, B.D. Freeman, Surface modification of water purification membranes, *Angew. Chem. Int. Ed.* 56 (2017) 4662–4711, <https://doi.org/10.1002/anie.201601509>.
- [2] R. Abejón, A. Garea, A bibliometric analysis of research on arsenic in drinking water during the 1992–2012 period: an outlook to treatment alternatives for arsenic removal, *J. Water Process Eng.* 6 (2015) 105–119, <https://doi.org/10.1016/j.jwpe.2015.03.009>.
- [3] G. Dong Kang, Y. Ming Cao, Development of antifouling reverse osmosis membranes for water treatment: a review, *Water Res.* 46 (2012) 584–600, <https://doi.org/10.1016/j.watres.2011.11.041>.
- [4] C. Liu, W. Wang, B. Yang, K. Xiao, H. Zhao, Separation, anti-fouling, and chlorine resistance of the polyamide reverse osmosis membrane: from mechanisms to mitigation strategies, *Water Res.* 195 (2021), 116976, <https://doi.org/10.1016/j.watres.2021.116976>.
- [5] S. Vetrivel, D. Rana, M.S. Sri Abirami Saraswathi, K. Divya, N.J. Kaleekkal, A. Nagendran, Cellulose acetate nanocomposite ultrafiltration membranes tailored with hydrous manganese dioxide nanoparticles for water treatment applications, *Polym. Adv. Technol.* 30 (2019) 1943–1950, <https://doi.org/10.1002/pat.4626>.
- [6] A. Pak, T. Mohammadi, Wastewater treatment of desalting units, *Desalination* 222 (2008) 249–254, <https://doi.org/10.1016/j.desal.2007.01.166>.
- [7] R.W. Field, G.K. Pearce, Critical, sustainable and threshold fluxes for membrane filtration with water industry applications, *Adv. Colloid Interface Sci.* 164 (2011) 38–44, <https://doi.org/10.1016/j.cis.2010.12.008>.
- [8] S. Shirazi, C.J. Lin, D. Chen, Inorganic fouling of pressure-driven membrane processes - a critical review, *Desalination* 250 (2010) 236–248, <https://doi.org/10.1016/j.desal.2009.02.056>.
- [9] D.M. Warsinger, S. Chakraborty, E.W. Tow, M.H. Plumlee, C. Bellona, S. Loutatidou, L. Karimi, A.M. Mikelonis, A. Achilli, A. Ghassemi, L.P. Padhye, S. A. Snyder, S. Curcio, C.D. Vecitis, H.A. Ararat, J.H. Lienhard, A review of polymeric membranes and processes for potable water reuse, *Prog. Polym. Sci.* 81 (2018) 209–237, <https://doi.org/10.1016/j.progpolymsci.2018.01.004>.
- [10] L.N. Sim, T.H. Chong, A.H. Taheri, S.T.V. Sim, L. Lai, W.B. Krantz, A.G. Fane, A review of fouling indices and monitoring techniques for reverse osmosis, *Desalination* 434 (2018) 169–188, <https://doi.org/10.1016/j.desal.2017.12.009>.
- [11] W. Guo, H.H. Ngo, J. Li, A mini-review on membrane fouling, *Bioreour. Technol.* 122 (2012) 27–34, <https://doi.org/10.1016/j.biortech.2012.04.089>.
- [12] I. Merino-García, S. Velizarov, New insights into the definition of membrane cleaning strategies to diminish the fouling impact in ion exchange membrane separation processes, *Sep. Purif. Technol.* 277 (2021), 119445, <https://doi.org/10.1016/j.seppur.2021.119445>.
- [13] J. Yin, B. Deng, Polymer-matrix nanocomposite membranes for water treatment, *J. Memb. Sci.* 479 (2015) 256–275, <https://doi.org/10.1016/j.memsci.2014.11.019>.
- [14] Y. He, D.M. Bagley, K.T. Leung, S.N. Liss, B.Q. Liao, Recent advances in membrane technologies for biorefining and bioenergy production, *Biotechnol. Adv.* 30 (2012) 817–858, <https://doi.org/10.1016/j.biotechadv.2012.01.015>.
- [15] C.Y. Tang, T.H. Chong, A.G. Fane, Colloidal interactions and fouling of NF and RO membranes: a review, *Adv. Colloid Interface Sci.* 164 (2011) 126–143, <https://doi.org/10.1016/j.cis.2010.10.007>.
- [16] D.M. Warsinger, S. Chakraborty, E.W. Tow, M.H. Plumlee, C. Bellona, S. Loutatidou, L. Karimi, A.M. Mikelonis, A. Achilli, A. Ghassemi, L.P. Padhye, S. A. Snyder, S. Curcio, C.D. Vecitis, H.A. Ararat, J.H. Lienhard, A review of polymeric membranes and processes for potable water reuse, *Prog. Polym. Sci.* 81 (2018) 209–237, <https://doi.org/10.1016/j.progpolymsci.2018.01.004>.
- [17] J. Wu, Z. Wang, Y. Wang, W. Yan, J. Wang, S. Wang, Polyvinylamine-grafted polyamide reverse osmosis membrane with improved antifouling property, *J. Memb. Sci.* 495 (2015) 1–13, <https://doi.org/10.1016/j.memsci.2015.08.007>.
- [18] Q. Wang, X. Wang, Z. Wang, J. Huang, Y. Wang, PVDF membranes with simultaneously enhanced permeability and selectivity by breaking the tradeoff effect via atomic layer deposition of TiO₂, *J. Memb. Sci.* 442 (2013) 57–64, <https://doi.org/10.1016/j.memsci.2013.04.026>.
- [19] S.H. Kim, S.Y. Kwak, B.H. Sohn, T.H. Park, Design of TiO₂ nanoparticle self-assembled aromatic polyamide thin-film-composite (TFC) membrane as an approach to solve biofouling problem, *J. Memb. Sci.* 211 (2003) 157–165, [https://doi.org/10.1016/S0376-7388\(02\)00418-0](https://doi.org/10.1016/S0376-7388(02)00418-0).
- [20] F. Zareei, S.M. Hosseini, A new type of polyethersulfone based composite nanofiltration membrane decorated by cobalt ferrite-copper oxide nanoparticles with enhanced performance and antifouling property, *Sep. Purif. Technol.* 226 (2019) 48–58, <https://doi.org/10.1016/j.seppur.2019.05.077>.
- [21] A. Abdel-Karim, S.H. Ismail, A.M. Bayoumy, M. Ibrahim, G.G. Mohamed, Antifouling PES/Cu@Fe₃O₄ mixed matrix membranes: quantitative structure–activity relationship (QSAR) modeling and wastewater treatment potentiality, *Chem. Eng. J.* 407 (2021), 126501, <https://doi.org/10.1016/j.cej.2020.126501>.
- [22] J.M. Luque-Alled, A. Abdel-Karim, M. Alberto, S. Leaper, M. Perez-Page, K. Huang, A. Vijayaraghavan, A.S. El-Kalliny, S.M. Holmes, P. Gorgojo, Polyethersulfone membranes: from ultrafiltration to nanofiltration via the incorporation of APTS functionalized-graphene oxide, *Sep. Purif. Technol.* 230 (2020), 115836, <https://doi.org/10.1016/j.seppur.2019.115836>.
- [23] T. Wang, J. Wang, Z. Zhao, X. Zheng, J. Li, H. Liu, Z. Zhao, Bio-inspired fabrication of anti-fouling and stability of nanofiltration membranes with a poly(dopamine)/graphene oxide interlayer, *Ind. Eng. Chem. Res.* (2021), <https://doi.org/10.1021/acs.iecr.1c03105>. A-P.
- [24] C. Ursino, R. Castro-Muñoz, E. Drioli, L. Gzara, M.H. Albeiruty, A. Figoli, Progress of nanocomposite membranes for water treatment, *Membranes (Basel)* 8 (2018) 1–40, <https://doi.org/10.3390/membranes8020018>.
- [25] M. Drobek, A. Figoli, S. Santoro, N. Navascués, J. Motuzas, S. Simone, C. Algieri, N. Gaeta, L. Querze, A. Trotta, G. Barbieri, R. Mallada, A. Julbe, E. Drioli, PVDF-MFI mixed matrix membranes as VOCs adsorbers, *Microporous Mesoporous Mater.* 207 (2015) 126–133, <https://doi.org/10.1016/j.micromeso.2015.01.005>.
- [26] A. Lejarazu-Larrañaga, Y. Zhao, S. Molina, E. García-Calvo, B. Van der Bruggen, Alternating current enhanced deposition of a monovalent selective coating for anion exchange membranes with antifouling properties, *Sep. Purif. Technol.* 229 (2019), 115807, <https://doi.org/10.1016/j.seppur.2019.115807>.
- [27] C. Fernandez-Gonzalez, B. Zhang, A. Domínguez-Ramos, R. Ibáñez, A. Irabien, Y. Chen, Enhancing fouling resistance of polyethylene anion exchange membranes using carbon nanotubes and iron oxide nanoparticles, *Desalination* 411 (2017) 19–27, <https://doi.org/10.1016/j.desal.2017.02.007>.
- [28] Z. Ali, Y. Wang, W. Ogieglo, F. Pacheco, H. Vovusha, Y. Han, I. Pinnau, Gas separation and water desalination performance of defect-free interfacially polymerized para-linked polyamide thin-film composite membranes, *J. Memb. Sci.* 618 (2021), 118572, <https://doi.org/10.1016/j.memsci.2020.118572>.
- [29] A. Lejarazu-Larrañaga, S. Molina, J.M. Ortiz, R. Navarro, E. García-Calvo, Circular economy in membrane technology: using end-of-life reverse osmosis modules for preparation of recycled anion exchange membranes and validation in electrodialysis, *J. Memb. Sci.* 593 (2020), 117423, <https://doi.org/10.1016/j.memsci.2019.117423>.
- [30] W. Lawler, J. Alvarez-Gaitan, G. Leslie, P. Le-Clech, Comparative life cycle assessment of end-of-life options for reverse osmosis membranes, *Desalination* 357 (2015) 45–54, <https://doi.org/10.1016/j.desal.2014.10.013>.
- [31] W. Lawler, Z. Bradford-Hartke, M.J. Cran, M. Duke, G. Leslie, B.P. Ladewig, P. Le-Clech, Towards new opportunities for reuse, recycling and disposal of used reverse osmosis membranes, *Desalination* 299 (2012) 103–112, <https://doi.org/10.1016/j.desal.2012.05.030>.
- [32] J. Wu, A.E. Contreras, Q. Li, Studying the impact of RO membrane surface functional groups on alginate fouling in seawater desalination, *J. Memb. Sci.* 458 (2014) 120–127, <https://doi.org/10.1016/j.memsci.2014.01.056>.
- [33] X. Wang, Y. Li, H. Li, C. Yang, Chitosan membrane adsorber for low concentration copper ion removal, *Carbohydr. Polym.* 146 (2016) 274–281, <https://doi.org/10.1016/j.carbpol.2016.03.055>.
- [34] M. Ben-Sasson, K.R. Zodrow, Q. Gengeng, Y. Kang, E.P. Giannelis, M. Elimelech, Surface functionalization of thin-film composite membranes with copper nanoparticles for antimicrobial surface properties, *Environ. Sci. Technol.* 48 (2014) 384–393, <https://doi.org/10.1021/es404232s>.
- [35] E.M.V. Hoek, A.K. Ghosh, X. Huang, M. Liong, J.I. Zink, Physical-chemical properties, separation performance, and fouling resistance of mixed-matrix ultrafiltration membranes, *Desalination* 283 (2011) 89–99, <https://doi.org/10.1016/j.desal.2011.04.008>.
- [36] X. Huang, K.L. Marsh, B.T. McVerry, E.M.V. Hoek, R.B. Kaner, Low-fouling antibacterial reverse osmosis membranes via surface grafting of graphene oxide, *ACS Appl. Mater. Interfaces* 8 (2016) 14334–14338, <https://doi.org/10.1021/acsami.6b05293>.
- [37] X. Li, Y. Liu, J. Wang, J. Gascon, J. Li, B. Van Der Bruggen, Metal-organic frameworks based membranes for liquid separation, *Chem. Soc. Rev.* 46 (2017) 7124–7144, <https://doi.org/10.1039/c7cs00575j>.
- [38] T. Li, Y. Ren, D. Wu, W. Zhang, M. Shi, C. Ji, L. Lv, M. Hua, W. Zhang, A novel water-stable two-dimensional zeolitic imidazolate frameworks thin-film composite membrane for enhancements in water permeability and nanofiltration

- performance, *Chemosphere* 261 (2020), <https://doi.org/10.1016/j.chemosphere.2020.127717>.
- [39] D.B. Mosqueda-Jimenez, P.M. Huck, Characterization of membrane foulants in drinking water treatment, *Desalination* 198 (2006) 173–182, <https://doi.org/10.1016/j.desal.2005.12.025>.
- [40] S.P. Nunes, A. Car, From charge-mosaic to micelle self-assembly: block copolymer membranes in the last 40 years, *Ind. Eng. Chem. Res.* 52 (2013) 993–1003, <https://doi.org/10.1021/ie202870y>.
- [41] W.S. Ang, M. Elimelech, Protein (BSA) fouling of reverse osmosis membranes: implications for wastewater reclamation, *J. Memb. Sci.* 296 (2007) 83–92, <https://doi.org/10.1016/j.memsci.2007.03.018>.
- [42] S. Ilyas, R. English, P. Aimar, J.F. Lahitte, W.M. de Vos, Preparation of multifunctional hollow fiber nanofiltration membranes by dynamic assembly of weak polyelectrolyte multilayers, *Colloids Surf. A Physicochem. Eng. Asp.* 533 (2017) 286–295, <https://doi.org/10.1016/j.colsurfa.2017.09.003>.
- [43] J. Wu, Z. Wang, Y. Wang, W. Yan, J. Wang, S. Wang, Polyvinylamine-grafted polyamide reverse osmosis membrane with improved antifouling property, *J. Memb. Sci.* 495 (2015) 1–13, <https://doi.org/10.1016/j.memsci.2015.08.007>.
- [44] H. Xie, J. Pan, B. Wei, J. Feng, S. Liao, X. Li, Y. Yu, Anti-fouling anion exchange membrane for electrodialysis fabricated by in-situ interpenetration of the ionomer to gradient cross-linked network of Ca-Na alginate, *Desalination* 505 (2021), 115005, <https://doi.org/10.1016/j.desal.2021.115005>.
- [45] X. Zheng, F. Zietzschmann, S. Plume, H. Paar, M. Ernst, Z. Wang, M. Jekel, Understanding and control of biopolymer fouling in ultrafiltration of different water types, *Water (Switzerland)* 9 (2017), <https://doi.org/10.3390/w9040298>.
- [46] M. Bortolini, M. Gamberi, C. Mora, F. Pilati, A. Regattieri, Design, prototyping, and assessment of a wastewater closed-loop recovery and purification system, *Sustainability* 9 (2017) 1938, <https://doi.org/10.3390/su9111938>.
- [47] S. Rezaei Soulegani, Z. Sherafat, M. Rasouli, Morphology, physical, and mechanical properties of potentially applicable coelectrospun polysulfone/chitosan-polyvinyl alcohol fibrous membranes in water purification, *J. Appl. Polym. Sci.* 138 (2021) 1–12, <https://doi.org/10.1002/app.49933>.
- [48] Q. Li, S. Mahendra, D.Y. Lyon, L. Brunet, M.V. Liga, D. Li, P.J.J. Alvarez, Antimicrobial nanomaterials for water disinfection and microbial control: potential applications and implications, *Water Res.* 42 (2008) 4591–4602, <https://doi.org/10.1016/j.watres.2008.08.015>.
- [49] A. Marcos-Madrazo, C. Casado-Coterillo, L. García-Cruz, J. Iniesta, L. Simonelli, V. Sebastián, M. del M. Encabo-Berzosa, M. Arruebo, Á. Irabien, Preparation and identification of optimal synthesis conditions for a novel alkaline anion-exchange membrane, *Polymers (Basel)* 10 (2018), <https://doi.org/10.3390/polym10080913>.
- [50] J. Pérez-Carvajal, P. Lalueza, C. Casado, C. Téllez, J. Coronas, Layered titanates JDF-L1 and AM-4 for biocide applications, *Appl. Clay Sci.* 56 (2012) 30–35, <https://doi.org/10.1016/j.clay.2011.11.020>.
- [51] C. Rubio, B. Murillo, C. Casado-Coterillo, A. Mayoral, C. Téllez, J. Coronas, A. Berenguer-Murcia, D. Cazorla-Amoros, Development of exfoliated layered stannosilicate for hydrogen adsorption, *Int. J. Hydrog. Energy* 39 (2014) 13180–13188, <https://doi.org/10.1016/j.ijhydene.2014.06.149>.
- [52] L. García-Cruz, C. Casado-Coterillo, J. Iniesta, V. Montiel, Á. Irabien, Chitosan: poly(vinyl) alcohol composite alkaline membrane incorporating organic ionomers and layered silicate materials into a PEM electrochemical reactor, *J. Memb. Sci.* 498 (2016) 395–407, <https://doi.org/10.1016/j.memsci.2015.08.040>.
- [53] M.I. Gutiérrez-Gutiérrez, D.F. Morales-Mendive, C.J. Muvdi-Nova, A. Chaves-Guerrero, Síntesis y caracterización de membranas híbridas a partir de quitosán, polivinil alcohol y sílice para su aplicación en deshidratación de gases, *Iteckne* 12 (2015) 33–43, <https://doi.org/10.15332/iteckne.v12i1.819>.
- [54] M. Higa, M. Kobayashi, Y. Kakiyama, A. Jikihara, N. Fujiwara, Charge mosaic membranes with semi-interpenetrating network structures prepared from a polymer blend of poly(vinyl alcohol) and polyelectrolytes, *J. Memb. Sci.* 428 (2013) 267–274, <https://doi.org/10.1016/j.memsci.2012.10.034>.
- [55] V. Freger, A. Bottino, G. Capannelli, M. Perry, V. Gitis, S. Belfer, Characterization of novel acid-stable NF membranes before and after exposure to acid using ATR-FTIR, TEM and AFM, *J. Memb. Sci.* 256 (2005) 134–142, <https://doi.org/10.1016/j.memsci.2005.02.014>.
- [56] M. Liu, Q. Chen, L. Wang, S. Yu, C. Gao, Improving fouling resistance and chlorine stability of aromatic polyamide thin-film composite RO membrane by surface grafting of polyvinyl alcohol (PVA), *Desalination* 367 (2015) 11–20, <https://doi.org/10.1016/j.desal.2015.03.028>.
- [57] J.A. Idarraga-Mora, A.S. Childress, P.S. Friedel, D.A. Ladner, A.M. Rao, S. M. Husson, Role of nanocomposite support stiffness on TFC membrane water permeance, *Membranes (Basel)* 8 (2018) 3–5, <https://doi.org/10.3390/membranes8040111>.
- [58] T. Takahashi, M. Imai, I. Suzuki, Water permeability of chitosan membrane involved in deacetylation degree control, *Biochem. Eng. J.* 36 (2007) 43–48, <https://doi.org/10.1016/j.bej.2006.06.014>.
- [59] C. Casado, D. Ambroj, Á. Mayoral, E. Vispe, C. Téllez, J. Coronas, Synthesis, swelling, and exfoliation of microporous lamellar titanate-silicate AM-4, *Eur. J. Inorg. Chem.* 4 (2011) 2247–2253, <https://doi.org/10.1002/ejic.201100152>.
- [60] R. Gerard, H. Hachisuka, M. Hirose, New membrane developments expanding the horizon for the application of reverse osmosis technology, *Desalination* 119 (1998) 47–55, [https://doi.org/10.1016/S0011-9164\(98\)00102-7](https://doi.org/10.1016/S0011-9164(98)00102-7).
- [61] B. Díez, N. Roldán, A. Martín, A. Sotto, J.A. Perdigón-Melón, J. Arsuaga, R. Rosal, Fouling and biofouling resistance of metal-doped mesostructured silica/polyethersulfone ultrafiltration membranes, *J. Memb. Sci.* 526 (2017) 252–263, <https://doi.org/10.1016/j.memsci.2016.12.051>.
- [62] M.S. Sri Abirami Saraswathi, D. Rana, K. Divya, S. Gowrishankar, A. Nagendran, Versatility of hydrophilic and antifouling PVDF ultrafiltration membranes tailored with polyhexanide coated copper oxide nanoparticles, *Polym. Test.* 84 (2020), <https://doi.org/10.1016/j.polymertesting.2020.106367>.
- [63] C. Casado-Coterillo, F. Andrés, C. Téllez, J. Coronas, Á. Irabien, Synthesis and characterization of ETS-10/chitosan nanocomposite membranes for pervaporation, *Sep. Sci. Technol.* 49 (2014) 1903–1909, <https://doi.org/10.1080/01496395.2014.908921>.
- [64] X. Zhu, X. Tang, X. Luo, X. Cheng, D. Xu, Z. Gan, W. Wang, L. Bai, G. Li, H. Liang, Toward enhancing the separation and antifouling performance of thin-film composite nanofiltration membranes: a novel carbonate-based preoccupation strategy, *J. Colloid Interface Sci.* 571 (2020) 155–165, <https://doi.org/10.1016/j.jcis.2020.03.044>.
- [65] Y. Yu, M. Liu, H. Huang, L. Zhao, P. Lin, S. Huang, J. Xu, H. Wang, L. Wang, Low cost fabrication of polypropylene fiber composite membrane with excellent mechanical, superhydrophilic, antifouling and antibacterial properties for effective oil-in-water emulsion separation, *React. Funct. Polym.* 142 (2019) 15–24, <https://doi.org/10.1016/j.reactfunctpolym.2019.05.010>.
- [66] H. Rabiee, M.H.D.A. Farahani, V. Vatanpour, Preparation and characterization of emulsion poly(vinyl chloride) (EPVC)/TiO₂ nanocomposite ultrafiltration membrane, *J. Memb. Sci.* 472 (2014) 185–193, <https://doi.org/10.1016/j.memsci.2014.08.051>.
- [67] M. Hu, Z. Cui, J. Li, L. Zhang, Y. Mo, D.S. Dlamini, H. Wang, B. He, J. Li, H. Matsuyama, Ultra-low graphene oxide loading for water permeability, antifouling and antibacterial improvement of polyethersulfone/sulfonated polysulfone ultrafiltration membranes, *J. Colloid Interface Sci.* 552 (2019) 319–331, <https://doi.org/10.1016/j.jcis.2019.05.065>.
- [68] N. Nasrollahi, S. Aber, V. Vatanpour, N.M. Mahmoodi, Development of hydrophilic microporous PES ultrafiltration membrane containing CuO nanoparticles with improved antifouling and separation performance, *Mater. Chem. Phys.* 222 (2019) 338–350, <https://doi.org/10.1016/j.matchemphys.2018.10.032>.
- [69] P. Kanagaraj, I.M.A. Mohamed, W. Huang, C. Liu, Membrane fouling mitigation for enhanced water flux and high separation of humic acid and copper ion using hydrophilic polyurethane modified cellulose acetate ultrafiltration membranes, *React. Funct. Polym.* 150 (2020), <https://doi.org/10.1016/j.reactfunctpolym.2020.104538>.
- [70] V. Vatanpour, S.S. Madaeni, R. Moradian, S. Zinadini, B. Astinchap, Novel antibiofouling nanofiltration polyethersulfone membrane fabricated from embedding TiO₂ coated multiwalled carbon nanotubes, *Sep. Purif. Technol.* 90 (2012) 69–82, <https://doi.org/10.1016/j.seppur.2012.02.014>.
- [71] F. Jamshaid, M.R. Dilshad, A. Islam, R.U. Khan, A. Ahmad, M. Adrees, B. Haider, Synthesis, characterization and desalination study of polyvinyl chloride-co-vinyl acetate/cellulose acetate membranes integrated with surface modified zeolites, *Microporous Mesoporous Mater.* 309 (2020), <https://doi.org/10.1016/j.micromeso.2020.110579>.
- [72] R. Singh, V.S.K. Yadav, M.K. Purkait, Cu₂O photocatalyst modified antifouling polysulfone mixed matrix membrane for ultrafiltration of protein and visible light driven photocatalytic pharmaceutical removal, *Sep. Purif. Technol.* 212 (2019) 191–204, <https://doi.org/10.1016/j.seppur.2018.11.029>.
- [73] H.Z. Shafi, A. Matin, S. Akhtar, K.K. Gleason, S.M. Zubair, Z. Khan, Organic fouling in surface modified reverse osmosis membranes: filtration studies and subsequent morphological and compositional characterization, *J. Memb. Sci.* 527 (2017) 152–163, <https://doi.org/10.1016/j.memsci.2017.01.017>.
- [74] E. Akhondi, F. Wicaksana, A.G. Fane, Evaluation of fouling deposition, fouling reversibility and energy consumption of submerged hollow fiber membrane systems with periodic backwash, *J. Memb. Sci.* 452 (2014) 319–331, <https://doi.org/10.1016/j.memsci.2013.10.031>.
- [75] G.M. Geise, Why polyamide reverse-osmosis membranes work so well, *Science* 371 (2021) 31–32, <https://doi.org/10.1126/science.abe9741> (80-).